Machine-learning models of coral cover and life histories reveal that climate refugia for coral reefs persist into 2050

Kyle J. A. Zawada[1], Emily S. Darling[2,*], Stacy D. Jupiter[2], Timothy R. McClanahan[2], Joseph M. Maina[1]

[1] School of Natural Sciences, Macquarie University, Sydney, Australia.
[2] Marine Program, Wildlife Conservation Society, Bronx, NY, USA.

[*] Corresponding author: edarling@wcs.org

Abstract

Climate change is accelerating the decline of coral reefs, yet some locations may retain conditions that support persistence under future warming. We compiled 45,091 coral field observations (1960–2025) and 42 climate, biophysical, and human-pressure predictors to train machine-learning ensembles that estimate coral cover in 2020 and 2050, and life-history composition in 2020, across a global high-resolution (250 m) dataset of suitable coral reef habitat (8.9 million pixels; 554,443 km^2). We then used a multi-objective optimization framework to identify reef areas that jointly maximize current and future coral cover, life-history diversity, spatial cohesion, and model certainty. Our results reveal 166,364 km² of climate-resilient reefs spanning 72 countries and 100 territories and jurisdictions, adding 30 countries and 54 jurisdictions beyond the original 50 Reefs assessment (Beyer et al. 2018). More than half of this resilient habitat (61%; 100,775 km^2) occurs within five countries with extensive reef systems: the Bahamas, Cuba, Australia, Indonesia, and the Philippines. These findings highlight the uneven but widespread distribution of potential climate refugia and emphasize the opportunity for countries to strategically focus national policies, conservation finance, and management actions on climate-resilient areas most likely to sustain coral reef futures.

Introduction

Coral reef ecosystems are experiencing unprecedented stress from increasingly frequent and severe marine heatwaves, driving widespread bleaching and mortality (Hughes et al 2017; Li and Donner 2022). These events have caused major losses in living coral cover (Hoegh-Guldberg et al 2023), reorganization of reef communities (McClanahan et al 2014; Hughes et al 2017), and declines in ecological functioning (Pratchett et al 2011). Recent global bleaching has exposed an estimated 68–84% of shallow tropical reefs to bleaching-level heat stress, highlighting rapidly shifting climate baselines (Spady et al 2026). Consequently, a prevailing narrative suggests coral reefs have passed climate-driven thresholds at 1.5ºC above historical baselines (Osland et al 2025; Lenton et al 2025), with projections indicating severe and widespread degradation under future warming scenarios (Frieler et al 2013; Cornwall et al 2021; Zeng et al 2025). Yet despite these forecasts, reef futures remain uncertain and

projections vary with data, model structures, and their analysis and assumptions (McClanahan and Azali 2021: Klein et al 2024).

Growing tension between global-scale risk projections and observed local persistence has elevated the importance of climate refugia in ecosystem and coral reef conservation. Evolutionary and ecological refugia are habitats where biodiversity can persist and potentially recover and expand after climatic threats have declined (Keppel et al 2012). Early work in coral reefs focused on conditions where corals avoid bleaching, such as areas with hydrodynamic cooling (Nakamura et al 2005; Schmidt et al 2016) and reduced solar irradiance from clouds or turbidity (Gonzalez-Espinosa and Donner 2021; Morais et al 2026; Sully and Van Woesik 2020). Recently, considerations of climate refugia have expanded to include not only areas that avoid climate stress, but also areas that can resist and recover, defined as an avoidance, resistance, recovery (ARR) framework of refugia (McClanahan et al 2024).

Global efforts to map coral reef climate refugia have primarily focused on identifying areas that avoid acute thermal and cyclone stress. A major advance was the '50 Reefs', which optimized the selection of large reef areas (500 km^2) projected to experience lower thermal stress and storm damage while maintaining strong larval connectivity (Beyer et al 2018; Hoegh-Guldberg et al 2018). This analysis has since guided more than US$100 million in conservation investments (Bloomberg Philanthropies 2021). However, environmental datasets available in 2018 were relatively coarse (5 km or 0.05° resolution, ~31 km^2) and the analysis did not integrate modifying variables such as oceanography or human pressures, factors known to strongly mediate local bleaching, coral mortality, and persistence (Loya et al 2001; Darling et al. 2019; MacNeil et al. 2019; McClanahan et al 2020; McClanahan 2023, 2025). In addition, Beyer et al. (2018) incorporated no empirical observations of coral cover or composition, limiting the ability to understand ecological patterns that underpin refugia. These limitations highlight the need for updated, higher-resolution assessments that incorporate a broader suite of ecological and environmental drivers to identify fine-scale climate refugia.

A next generation of refugia mapping therefore requires empirical measures of coral condition, including total coral cover and life-history strategies, to ground truth models with biological mechanisms that shape persistence. Total percent live coral cover is a composite metric aggregating many scleractinian coral taxa whose relative abundance influences the outcomes of heat and other climate change threats. Nevertheless, coral cover is the most frequently measured variable and likely reflects cumulative impacts, resistance, and recovery potential needed to support key ecological functions and services (Perry et al 2013; Beck et al 2022). Coral assemblage composition captures functional differences influencing adaptation, resistance, and recovery. Pooling taxa into competitive, stress-tolerant, and weedy life-history strategies provides a useful framework for interpreting resilience (Darling et al 2012; Darling et al 2013). Dominance by large branching and plating competitive corals can indicate avoidance refugia; stress-tolerant assemblages of massive corals often signal resistance; and communities dominated by fast-growing weedy taxa typically support rapid recovery. Together, these life-history patterns help identify three climate-refugia types: avoidance, resistance, and recovery (ARR; McClanahan et al. 2024). While observations to coral genera are less commonly recorded than total coral cover, modelling coral life histories can provide a

mechanistic foundation for identifying ARR refugia by revealing how different functional strategies contribute to persistence under future climate stress.

Here, we aim to identify contemporary and future climate refugia for coral reefs using machine learning and multi-objective prioritization that combines empirical coral cover and life history observations with environmental datasets and spatial optimization. Our framework also leverages high-resolution reef extent maps (e.g., Lyons et al 2024) and incorporates model uncertainty to identify suitable locations for coral resilience at high resolution (250 m), which can provide critical information to complement local knowledge and decision-making to ensure the persistence of ecological services to tropical reef stakeholders. Our goals are to: (1) model the current and future environmental conditions that influence coral cover and life history composition; (2) prioritize climate refugia using multi-objective optimization and an ARR resilience framework; and (3) evaluate outcomes across global, regional, and national scales to inform conservation decision-making.

Methods

The full workflow is summarized in Figure 1.

Empirical observations and predictor variables

We compiled a global dataset of coral-reef ecological surveys conducted between 1960 and 2025 including 37,716 observations of total coral cover, of which 7,375 observations include coral genera abundance that can be classified into competitive, weedy, and stress-tolerant life-history groups (Fig. S1). Surveys were drawn from long-term monitoring programs, academic and government studies, published datasets, and other publicly available sources (Table S1). Observations were retained only if they fell within mapped reef extent from the Allen Coral Atlas (2022; https://allencoralatlas.org/) or the UNEP-WCMC Global Distribution of Coral Reefs (UNEP-WCMC et al 2021). Coral life-history composition and its relationship to avoidance, resistance, and recovery (ARR) refugia followed Darling et al (2012, 2019) and McClanahan et al (2024) (Table S2). We removed observations when essential predictors were missing; depth was most frequently absent and could not be reliably imputed in shallow, complex coastal settings.

Environmental and anthropogenic predictors included 42 variables representing ocean temperature, chemistry, geomorphology, connectivity, and human pressure (see Supporting Information; Table S3). Sea surface temperature (SST) metrics captured both central tendencies and variability, including chronic long-term climatologies and 6-year windows preceding each survey year to represent background conditions and recent disturbances (McClanahan et al 2019). Additional predictors described chemistry (e.g. calcite, nutrients, dissolved oxygen, pH), light availability (PAR, Kd, benthic light), and modifying variables (e.g., depth, slope, ruggedness, geomorphic zones). These data combined static layers (e.g. human gravity, sediment plumes, connectivity) and time-varying layers derived from a diversity of sources and spatial resolutions (Table S3).

Our modelling framework extends the global climate-refugia assessment of Beyer et al (2018) by explicitly incorporating empirical coral cover and life-history composition and a broader suite of environmental domains. Whereas the original 50 Reefs analysis focused primarily on excess heat, cyclone exposure, and larval connectivity, we integrate these drivers alongside a broader set of climate, oceanographic, and human pressure predictors with documented links to coral assemblages (e.g. McClanahan and Azali 2021; Table S3). By directly training machine learning models for total coral cover and life history abundance with these variables, we improve the ecological grounding and spatial resolution of climate refugia predictions based on the direct modelling of present and future coral cover and composition.

Model development and training

All predictors were harmonized to a global 250 m × 250 m reef grid created by rasterizing and combining the Allen Coral Atlas (5 m) and UNEP-WCMC reef-extent datasets. The resulting mask comprised 8,871,088 reef pixels (554,443 km^2). Resampling introduced minor boundary deviations, especially along sharp coastlines and environmental gradients, but ensured that all predictors were aligned at a common resolution. Because effective model resolution is governed by the coarsest input layer, fine-scale predictions inherit the grain of underlying predictors rather than the 250 m output grid (see Table S3). Predictors were screened for multicollinearity using variance inflation factors (VIF < 7), yielding non-collinear feature sets for model training.

We modelled total hard coral cover and the cover of competitive, weedy, and stress-tolerant life histories using XGBoost gradient tree boosting (Chen and Guestrin 2016). Coral province was included as a categorical predictor to capture broad biogeographic structure. To reduce spatial and temporal autocorrelation, surveys were grouped into spatiotemporal bins of ~11 km and five years. Bins were randomly assigned to training (50%), validation (25%), or test (25%) sets using a three-way holdout (Raschka et al 2018). This procedure was repeated independently for 100 model runs per response variable (n = 4 responses). Models were trained with early stopping based on validation error, and hyperparameters were tuned within constrained ranges for tree depth, learning rate, subsampling, and regularization. In total, 400 gradient-boosting models (100 per response) were trained to quantify predictive robustness and variability.

Identifying drivers of coral cover and composition

We interpreted variable importance and effect direction using Shapley Additive Explanations (SHAP; Lundberg et al 2019), which decompose model predictions into additive contributions from individual predictors while accounting for interactions and correlated features. For each model we computed mean absolute SHAP values to summarize variable influence and examined SHAP–predictor correlations to determine effect direction. Conditional SHAP dependence plots were used to visualize nonlinear and threshold relationships while conditioning on the remaining predictors. Ensemble SHAP patterns were then used to characterise global drivers of total coral cover and life-history abundance.

Model performance assessment and prediction

For each response variable, model performance was evaluated against a mean-only null model across 100 runs, using mean absolute error (MAE) and median absolute deviation (MAD). We defined skill as the proportional reduction in MAE or MAD relative to the null and required at least 10% improvement for a model to be retained. Paired permutation tests by coral province assessed whether skill exceeded this threshold. Only models meeting these criteria contributed to spatial predictions, allowing model sets to differ among provinces. Final ensembles were used to predict coral cover and life-history cover for all reef cells globally at 250 m resolution for 2020 and 2050. Future predictions used CMIP6 SSP5-8.5 forcing (Eyring et al 2016), selected as a severe, but widely used, mid-century climate scenario.

Spatial optimization of climate refugia

For spatial optimization, we aggregated 250 m predictions to 5 km^2 (2.24 km × 2.24 km) planning units. Percent cover for total coral and each life-history group was converted to absolute coral area (km^2) per 250 m pixel and summed within each 5 km^2 planning unit (80 x 250 m pixels per planning unit). Reef prioritisation was formulated as a binary integer linear program in which each 5 km^2 planning unit was a decision variable (1 = selected, 0 = excluded) under a fixed 30% area budget applied independently per marine ecoregion, consistent with Kunming–Montreal Global Biodiversity Framework Target 3 (CBD 2022). The model jointly optimized across four complementary objectives (equations provided in Appendix 1):

1. Present and future total coral cover. We maximize a blended measure of present (weights β = 0.7, 2020) and projected future coral cover (weights γ = 0.3, 2050) to prioritize existing biological capital while also addressing expected persistence. Each reef cell receives a score based on its current absolute coral cover and its expected future cover under climate projections, weighted to reflect the desired balance between immediate condition and long-term persistence.

2. Spatial cohesion. This objective rewards spatially clustered selections to promote compact, connected reef networks. Cohesion is quantified using a k-nearest-neighbour metric of the planning unit locations with distance-decay weighting, such that planning units embedded within dense clusters are more desirable than isolated planning units. This encourages ecologically coherent portfolios of suitable reef areas that can support ecological processes and are more feasible to manage, rather than fragmented, dispersed selections.

3. Coral life history representation and diversification. This ensures representation across coral life-history strategies (competitive, stress-tolerant, and weedy taxa), analogous to portfolio diversification across ARR climate refugia types (McClanahan et al 2024). For each 5 km^2 planning unit, absolute area (km^2) of competitive, stress-tolerant and weedy cover in 2020 was used to indicate life history representation. A square-root transformation was applied to introduce diminishing returns, preventing over-allocation to already well-represented life histories. Weights were optionally adjusted by

ecoregion-level rarity, defined using density thresholds, to prioritize rare life histories while maintaining balanced portfolio composition in each ecoregion.

4. Risk minimization. We minimize ecological risk using an *a priori* composite risk score that penalizes reefs with high predictive uncertainty across 100 ensemble model runs in 2020 and 2050 (70% weight) and reefs projected to experience proportional declines in coral cover between 2020 and 2050 (30% weight). Uncertainty is calculated as a coefficient-of-variation–style ratio (standard deviation relative to mean cover) for each time period and combined across years. Decline is defined as proportional loss between time periods (gains are not penalized). These components are combined into a per-site risk score and summed across selected reefs to produce portfolio-level risk.

All optimisations were solved using the Gurobi Optimizer (Gurobi Optimization LLC 2026) with lexicographic multi-objective settings and standard mixed-integer programming controls (e.g. time limits, MIP gap, number of threads). Planning unit selections were then downscaled to 250 m by assignments of all constituent reef pixels within 5 km² planning units. Prioritised and non-prioritised reef pixels were intersected with Exclusive Economic Zones (EEZs) and protected area polygons (UNEP and IUCN 2026) to evaluate patterns across national jurisdictions, protected areas and other effective area-based conservation measures (OECMs). We also compared results with the original Beyer et al (2018) portfolio. Sensitivity analyses mapped z-scores for each objective and selection frequencies across weighting scenarios to assess robustness and highlight consistently selected priority areas.

Results and Discussion

Suitable coral reef habitat

After combining two global coral reef habitat maps, we identified 554,443 km^2 of suitable coral habitat at 250 m resolution that we assessed for characteristics of climate resilience. Our total habitat estimate is substantially greater than previous estimates, such as the high-resolution estimate of 348,361 km^2 of shallow coral reefs (Lyons et al 2024, Allen Coral Atlas 2022) and previous global coral reef area estimates of 249,713 km^2 (Burke et al 2012) and 284,300 km^2 (UNEP-WCMC et al 2021). However, past validation of reef area estimates suggests ~80% accuracy when the lowest reef resolution of ~200 km^2 was used (Lyons et al 2020), and 20-67% accuracy was reported for Allen Coral Atlas maps in New Caledonia driven by coral/algae class merging and sparse field training data (Andréfouët et al 2024). Notably, an early estimate of reef area using a 1° x 1° (or, 100 x 100 km) global grid and environmental data provide a value more similar to ours at ~600,000 km^2 (ReefBase 1996 *sensu* Kleypas et al 1999). Therefore, environmental data may select a higher value than satellite-based reef detection methods.

In addition, other factors likely explain differences in estimated coral reef habitat area: (1) earlier efforts used coarser spatial resolutions that could fail to detect small reefs, compared to our mapping of 250 m resolution; (2) suitable environmental habitat for realized coral

occurrence may exceed satellite-mapped carbonate substrate that can be limited by depth (e.g., 15 m depth limit in Lyons et al 2024); and (3) we used an "or" operator when aggregating the two coral layers: pixels classified as coral in either the Allen Coral Atlas (2022) or UNEP-WCMC et al (2021) dataset were retained in our 250 m extent grid. This inclusive approach captures all potential reef habitat, whereas an "and" operator would have produced a more conservative estimate. However, our method has likely identified habitat locations that may not be geologically suitable for coral growth, such as soft substrate (sand or seagrass) habitat. Therefore, the ecological differences between the fundamental and realized coral ecological niche or habitat and the predictive accuracy of these two niche spaces will require future ground-truthing (e.g., Andréfouët et al (2024).

Predictive modelling and performance

Machine-learning models to predict percent coral cover and the life history cover of competitive, stress tolerant, and weedy life histories globally showed reasonable explanatory power during training but lower performance in independent tests. Across responses, independent testing R^2 ranged from 0.08–0.28, and MAE from 3–13%, with low variation across the 100-run ensemble indicating stable results (Table S4). Total coral cover had the highest R^2 (0.28) but also the largest error (12.9%; Table S4). Performance declined for life history groups, which is expected with fewer observations and occurrences over a smaller value range giving the models less variation to learn from. The proportion of XGBoost models meeting accuracy and significance thresholds varied widely among provinces and coral responses (Fig. S2; Table S5); areas with poor performance likely represent regions with insufficient field data. Where no models passed thresholds, predictions relied on supervised learning from global datasets.

Drivers of coral cover and composition

SHAP summaries and partial dependence plots (Fig. 2, Fig. S3) highlighted consistent predictors of coral cover, including temperature variability and extreme heat, distance from 500 m depth, light, cyclone maximum wind speed, and connectivity. The response relationships show clear declines in coral cover with increasing SST variability (SD, skewness) and acute extreme heat (DHW, 6 years), maximum cyclone strength, and light. Coral cover also increases with some variables, including SST 0.9 quantile, distance from 500 m depth (deep water), and connectivity. Non-linear responses are common (Fig. S3) and include some important variables, such as temperature mean, kurtosis, and standard deviation, cyclones, light, distance from 500 m depth, sediments, calcite, and cyclones metrics. These results are generally supported by previous studies but they also indicate some local and subregional patterns of interest for improving local models (McClanahan and Sola 2024). For example, McClanahan (2025) summarizes 15 machine learning coral reef studies and suggests broad agreement on the core variables (e.g. temperature mean, skewness, kurtosis, excess heat, depth, light, dissolved oxygen, calcite, and human presence), the importance of modifying variables, and some differences based on locations and the specific coral reef metric.

Life history analysis indicates weaker fits to models, although relationships to specific predictor variables are consistent with ecological theory. For example, sensitive competitive corals were negatively affected by human gravity (a proxy for fishing pressure, Cinner et al 2018), depth, and temperature. In contrast, weedy corals correlated positively with human gravity, cyclone wind speed, light, sedimentation, and several SST metrics, reflecting their opportunistic disturbance-driven traits (Darling et al 2012, 2013; Zinke et al 2018). Stress-tolerant corals were also negatively affected by temperature and environmental conditions (light, depth) but increased in abundance with some extreme heat metrics (SST 0.9 quantile) consistent with their replacement of more sensitive corals over repeated bleaching events (Darling et al 2019, McClanahan et al 2024). The presence of climate, environmental, biophysical, and human pressure predictors across models of different coral traits and life histories underscores complex, nonlinear coral responses (McClanahan et al, 2025; Zinke et al 2018).

Spatial prioritization of climate refugia and implications for conservation

Predicted patterns of 2020–2050 coral cover and ARR refugia informed the optimized selection of climate-resilient reef areas (Fig. 3). Selected sites scored higher across all portfolio objectives (Fig. 4), and spatial Z-score distributions show how objective variability shaped outcomes (Fig. S4). The full 250 m global prioritization surface underlying the portfolio analysis is publicly available as a GeoTIFF (Zawada et al 2026) corresponding to the optimized solution (https://doi.org/10.5281/zenodo.18686274).

From the 554,443 km² of suitable coral reef habitat, our prioritization identified 166,364 km^2 of climate-resilient reefs across 72 countries and 100 territories and jurisdictions (Fig. 5; Table S6). This represents 128,788 km² of newly identified priority areas relative to Beyer et al. (2018), which identified 148,547 km² across 42 countries and 46 territories and jurisdictions. Only 37,576 km² overlap between the two analyses, indicating substantial expansion and refinement of global climate-resilient reef portfolios with our analysis, i.e., the '50 Reefs plus' (Table S6).

More than half of the new priority areas (100,755 km^2, or 60.3%) occur in five countries: the Bahamas (32,105 km^2), Cuba (18,914 km^2), Australia (18,390 km^2), Indonesia (16,150 km^2), and the Philippines (15,196 km^2). Small island territories have the highest proportion of selected reef areas: Niue (31 km^2 of 40 km^2), Vanuatu (1,403 km^2 of 2,007 km^2), American Samoa (88 km^2 of 129 km²), Comores (271 km^2 of 405 km^2), Christmas Island (16 km^2 of 25 km^2), and the Chagos Archipelago (1,816 km^2 of 2,880 km^2) each have more than 60% of their national or territorial reef extent selected as priority climate refugia.

The Atlantic–Caribbean shows some of the most substantial gains when refugia criteria are expanded beyond thermal-stress avoidance to include reefs that can resist and recover from bleaching. Our analysis identifies extensive new potential refugia not captured by Beyer et al. (2018), including 1,497 km^2 of resilient reef in Belize (45% of national reef extent), 1,480 km^2 in the Turks and Caicos Islands (28%), 1,101 km^2 in Panama (53%), and 417 km^2 in Nicaragua (43%). These results indicate that the Caribbean may harbour greater resilience potential than

previously recognised, offering renewed opportunities to support coral reef futures in a region long viewed as highly vulnerable (see also Chollett et al 2022).

Other notable marine areas that are included in the 50 Reefs plus analysis compared to the Beyer et al. (2018) include New Caledonia (2,011 km^2, or 21.1% of national or territorial reef extent), the Chagos archipelago (1,816km^2, or 63.1%), Vanuatu (1,403 km^2, or 69.9%), Micronesia (1,448 km^2, or 28.5%), Palau (640 km^2, or 34.0%), and the Galapagos islands (205 km2, or 30.1%).

Of the 166,364 km^2 identified as climate-resilient coral reefs, 120,354 km^2 (72.3%) fall within areas currently reported as protected areas or OECMs (UNEP-WCMC and IUCN 2026). However, many protected and managed areas are under-resourced and "paper parks," limiting their ability to deliver ecological and social benefits (Gill et al 2017; Stephenson et al 2025). The finding that most priority areas already lie within some form of designated protection suggests that ensuring effective management could secure much of the global climate-resilient reef portfolio. The remaining 46,768 km^2 outside protected areas or OECMs (UNEP-WCMC and IUCN 2026) represents important opportunities for inclusion in national planning priorities, especially as Parties to the Convention on Biological Diversity expand area-based conservation to meet Target 3 of the Kunming–Montreal Global Biodiversity Framework by 2030.

Limitations and future directions

Several limitations should be considered when interpreting these results. First, the machine-learning models capture statistical rather than mechanistic relationships and thus assume that historical driver–response patterns will continue under future climate conditions. This may underestimate novel future states. Predictor datasets also vary in spatial and temporal resolution, for example, cyclone exposure layers (~200 km) are much coarser than habitat maps (250 m) which can mask fine-scale drivers of resilience. In addition, monitoring data are unevenly distributed across provinces (Fig. S1), and model performance was lowest in regions with sparse field observations (e.g., Tonga-Samoa; Table S5) and particularly for many life history models. These issues underscore the need for more standardized monitoring data, locally calibrated models that incorporate site-specific processes and coral adaptations (McClanahan and Sola 2024), and flexible objective functions that can be adjusted to regional model performance or desired custom weightings by stakeholders. Model structure and parameter choices can also influence outcomes, a pattern documented across coral-reef machine-learning studies (McClanahan 2025).

Second, the prioritization does not incorporate governance feasibility, management capacity, or implementation costs, factors that ultimately determine whether climate-resilient reefs can be effectively conserved and managed. For example, many protected and managed areas remain under-resourced (Gill et al 2017; Stephenson et al 2025), and assessing conditions of socioeconomic and political enabling conditions, compliance and enforcement, and long-term sustainable financing for conservation will be key to enduring ecological outcomes in these critical areas of climate resilience.

Looking forward, several refinements would strengthen future refugia assessments: integrating higher-resolution environmental predictors (e.g., water quality, hydrodynamics), using hierarchical and transfer-learning approaches to leverage local datasets, more monitoring information available for coral genera and life history abundance, and updating prioritizations iteratively as climate conditions and monitoring information evolve. Despite these constraints, the framework provides an improved and scalable global framework for identifying climate resilient reefs. Coupled with local knowledge, adaptive management, and national policies, these results can help guide durable conservation actions that support coral-reef ecosystem services into the mid-century.

Conclusions

This study shows that combining empirical coral reef observations with machine-learning predictions and multi-objective spatial optimization substantially improves the identification of climate refugia at global scale. By integrating present and projected persistence of coral cover alongside life-history diversity and representation, we provide the first high-resolution assessment of where reefs are most likely to endure severe mid-century warming. Despite widespread and increasing thermal stress, we find large and spatially distinct areas with ecological and environmental conditions that support coral reef persistence. These priority areas are concentrated in a subset of countries but occur across most reef regions, highlighting opportunities to strategically align conservation and management actions to the places offering the greatest long-term ecological and societal returns.

References

Allen Coral Atlas 2022 Imagery, maps and monitoring of the world's tropical coral reefs Zenodo (doi: 10.5281/zenodo.3833242)

Andréfouët S, Maële B, Stéphane G and Antoine G 2024 Evaluation of the Allen Coral Atlas benthic habitat map product for New Caledonia using representative habitat observations from a multi-species fishery assessment *Coral Reefs* **43** 523–540 (doi: 10.1007/s00338-024-02481-0)

Beck M W, Heck N, Narayan S, Menéndez P, Reguero B G, Bitterwolf S, Torres-Ortega S, Lange G-M, Pfliegner K, Pietsch McNulty V and Losada I J 2022 Return on investment for mangrove and reef flood protection *Ecosyst. Serv.* **56** 101440

Beyer H L, Kennedy E V, Beger M et al 2018 Risk-sensitive planning for conserving coral reefs under rapid climate change *Conserv. Lett.* **11** e12587 (doi: 10.1111/conl.12587)

Bloomberg Philanthropies 2021 50 Reefs Landscape Assessment: Progress, Lessons Learned, and Future Opportunities (Bloomberg Philanthropies Vibrant Oceans Initiative)

Burke L, Reytar K, Spalding M and Perry A 2011 *Reefs at Risk Revisited: Technical Notes on Modeling Threats to the World's Coral Reefs* (Washington, DC: World Resources Institute)

CBD 2022 Kunming–Montreal Global Biodiversity Framework... Secretariat of the Convention on Biological Diversity, Montreal, Canada

Chen T and Guestrin C 2016 XGBoost: a scalable tree boosting system *Proc. 22nd ACM SIGKDD Int. Conf. Knowledge Discovery and Data Mining* (New York: ACM) pp 785–794 (doi: 10.1145/2939672.2939785)

Chollett I, Escovar-Fadul X, Schill S R, Croquer A, Dixon A M, Beger M, Shaver E, Pietsch McNulty V and Wolff N H 2022 Planning for resilience: incorporating scenario and model uncertainty and trade-offs when prioritizing management of climate refugia *Glob. Change Biol.* **28** 4054–4068

Cinner J E, Maire E, Huchery C, MacNeil M A, Graham N A J, Mora C, McClanahan T R, Barnes M L, Kittinger J N, Hicks C C, D'Agata S et al 2018 Gravity of human impacts mediates coral reef conservation gains *Proc. Natl Acad. Sci. USA* **115** E6116–E6125

Cornwall C E, Comeau S, Kornder N A, Perry C T, van Hooidonk R, DeCarlo T M, Pratchett M S, Anderson K D, Browne N and Carpenter R 2021 Global declines in coral reef calcium carbonate production under ocean acidification and warming *Proc. Natl Acad. Sci. USA* **118** e2015265118

Darling E S, Alvarez-Filip L, Oliver T A, McClanahan T R and Côté I M 2012 Evaluating life-history strategies of reef corals from species traits *Ecol. Lett.* **15** 1378–1386

Darling E S, McClanahan T R and Côté I M 2013 Life histories predict coral community disassembly under multiple stressors *Glob. Change Biol.* **19** 1930–1940

Darling E S, McClanahan T R, Maina J et al 2019 Social–environmental drivers inform strategic management of coral reefs in the Anthropocene *Nat. Ecol. Evol.* **3** 1341–1350

Eyring V, Bony S, Meehl G A, Senior C A, Stevens B, Stouffer R J and Taylor K E 2016 Overview of the Coupled Model Intercomparison Project Phase 6 (CMIP6) experimental design and organization *Geosci. Model Dev.* **9** 1937–1958 (doi: 10.5194/gmd-9-1937-2016)

Frieler K, Meinshausen M, Golly A, Mengel M, Lebek K, Donner S D and Hoegh-Guldberg O 2013 Limiting global warming to 2 °C is unlikely to save most coral reefs *Nat. Clim. Change* **3** 165–170

Game E T, Bode M, McDonald-Madden E, Grantham H S and Possingham H P 2009 Dynamic marine protected areas can improve the resilience of coral reef systems *Ecol. Lett.* **12** 1336–1346

Gill D A, Mascia M B, Ahmadia G N, Glew L, Lester S E, Barnes M, Craigie I, Darling E S, Free C M, Geldmann J and Holst S 2017 Capacity shortfalls hinder the performance of marine protected areas globally *Nature* **543** 665–669

Gonzalez-Espinosa P C and Donner S D 2021 Cloudiness reduces the bleaching response of coral reefs exposed to heat stress *Glob. Change Biol.* **27** 3474–3486

Graham N A, Wilson S K, Benkwitt C E, Bonne R, Govinden R and Robinson J P 2024 Increased resilience and a regime shift reversal through repeat mass coral bleaching *Ecol. Lett.* **27** e14454

Gurobi Optimization LLC 2026 Gurobi Optimizer Reference Manual (https://www.gurobi.com)

Hoegh-Guldberg O, Skirving W, Dove S G, Spady B L, Norrie A, Geiger E F, Liu G, De La Cour J L and Manzello D P 2023 Coral reefs in peril in a record-breaking year *Science* **382** 1238–1240

Hoegh-Guldberg O, Kennedy E V, Beyer H L, McClennen C and Possingham H P 2018 Securing a long-term future for coral reefs *Trends Ecol. Evol.* **33** 936–944

Hughes T P, Kerry J T, Álvarez-Noriega M et al 2017 Global warming and recurrent mass bleaching of corals *Nature* **543** 373–377

Keppel G, Van Niel K P, Wardell-Johnson G W, Yates C J, Byrne M, Mucina L, Schut A G T, Hopper S D and Franklin S E 2012 Refugia: identifying and understanding safe havens for biodiversity under climate change *Glob. Ecol. Biogeogr.* **21** 393–404

Klein S G, Roch C and Duarte C M 2024 Systematic review of the uncertainty of coral reef futures under climate change *Nat. Commun.* **15** 2224

Kleypas J A, McManus J W and Meñez L A 1999 Environmental limits to coral reef development: where do we draw the line? *Am. Zool.* **39** 146–159

Lenton T M, Milkoreit M, Willcock S et al (eds) 2025 The Global Tipping Points Report 2025 University of Exeter, UK

Li X and Donner S D 2022 Lengthening of warm periods increased the intensity of warm-season marine heatwaves over the past 4 decades *Clim. Dyn.* **59** 2643–2654

Loya Y, Sakai K, Yamazato K, Nakano Y, Sambali H and van Woesik R 2001 Coral bleaching: the winners and the losers *Ecol. Lett.* **4** 122–131

Lundberg S M, Erion G G and Lee S-I 2019 Consistent individualized feature attribution for tree ensembles *arXiv* 1802.03888

Lyons M B, Murray N J, Kennedy E V et al 2024 New global area estimates for coral reefs from high-resolution mapping *Cell Rep. Sustain.* **1** 100015

Lyons M B, Roelfsema C M, Kennedy E V et al 2020 Mapping the world's coral reefs using a global multiscale earth observation framework *Remote Sens. Ecol. Conserv.* **6** 557–568

MacNeil M A, Mellin C, Matthews S, Wolff N H, McClanahan T R, Devlin M, Drovandi C, Mengersen K and Graham N A J 2019 Water quality mediates resilience on the Great Barrier Reef *Nat. Ecol. Evol.* **3** 620–627 (doi: 10.1038/s41559-019-0832-3)

Markowitz H 1952 Portfolio selection *J. Finance* **7** 77–91

McClanahan T, Darling E, Maina J, Muthiga N, D'Agata S, Leblond J, Arthur R, Jupiter S, Wilson S, Mangubhai S, Ussi A, Guillaume M, Humphries A, Patankar V, Shedrawi G, Pagu J and Grimsditch G 2020 Highly variable taxa-specific coral bleaching responses to thermal stresses *Mar. Ecol. Prog. Ser.* **648** 135–151

McClanahan T R, Azali M K, Muthiga N A et al 2024 Complex multivariate model predictions for coral diversity with climatic change *Ecosphere* **15** e70057

McClanahan T R, Darling E S, Maina J M, Muthiga N A, D'Agata S D, Jupiter S D, Arthur R, Wilson S K, Mangubhai S, Nand Y and Ussi A M 2019 Temperature patterns and mechanisms influencing coral bleaching during the 2016 El Niño *Nat. Clim. Change* **9** 845–851 (doi: 10.1038/s41558-019-0563-8)

McClanahan T R 2025 Evaluating coral reef hazards requires both explanatory and predictive models *Coral Reefs* (doi: 10.1007/s00338-025-02770-3)

McClanahan T R 2023 Local heterogeneity of coral reef diversity and environmental stress provides opportunities for small-scale conservation *Divers. Distrib.* **29** 1324–1340

McClanahan T R and Azali M K 2021 Environmental variability and threshold model's predictions for coral reefs *Front. Mar. Sci.* **8** 778121

McClanahan T R and Sola E 2024 Comparing modeled predictions of coral reef diversity along a latitudinal gradient in Mozambique *Front. Ecol. Evol.* **12** 1450383

Morais J, Almeida P M, Avelino C D et al 2026 Risk or relief? The influence of river plumes on coral bleaching and disease *Mar. Pollut. Bull.* **222** 118741

Nakamura T, Van Woesik R and Yamasaki H 2005 Photoinhibition of photosynthesis is reduced by water flow in the reef-building coral *Acropora digitifera Mar. Ecol. Prog. Ser.* **301** 109–118

Osland M J, Bradford J B, Toth L T et al 2025 Ecological thresholds and transformations due to climate change: the role of abiotic stress *Ecosphere* **16** e70229

Perry C T, Murphy G N, Kench P S et al 2013 Caribbean-wide decline in carbonate production threatens coral reef growth *Nat. Commun.* **4** 1402

Polasky S 2008 Why conservation planning needs socioeconomic data *Proc. Natl Acad. Sci. USA* **105** 6505–6506

Pratchett M S, Hoey A S, Wilson S K, Messmer V and Graham N A J 2011 Changes in biodiversity and functioning of reef fish assemblages following coral bleaching and coral loss *Diversity* **3** 424–452

Raschka S 2018 Model evaluation, model selection, and algorithm selection in machine learning *arXiv* 1811.12808

ReefBase 1996 ReefBase: a global database of coral reefs and their resources ICLARM, Manila, Philippines

Schmidt G M, Wall M, Taylor M, Jantzen C and Richter C 2016 Large-amplitude internal waves sustain coral health during thermal stress *Coral Reefs* **35** 869–881

Spady B L, Skirving W J, De La Cour J L et al 2026 The 4th global coral bleaching event: ushering in an era of near-annual bleaching *Coral Reefs* (doi: 10.1007/s00338-025-02810-x)

Spalding M D, Fox H E, Allen G R et al 2007 Marine ecoregions of the world: a bioregionalization of coastal and shelf areas *Bioscience* **57** 573–583

Stephenson F *et al* 2025 Quality of marine protected areas is critical to achieving global biodiversity targets *npj Ocean Sustain.* **4** 63 (https://doi.org/10.1038/s44183-025-00169-8)

Sully S and van Woesik R 2020 Turbid reefs moderate coral bleaching under climate-related temperature stress *Glob. Change Biol.* **26** 1367–1373

UNEP-WCMC, WorldFish Centre, WRI and TNC 2021 Global distribution of coral reefs Version 4.1 UNEP-WCMC, Cambridge, UK (doi:10.34892/t2wk-5t34)

UNEP-WCMC and IUCN 2026 Protected Planet: The World Database on Protected Areas (WDPA) and World Database on Other Effective Area-based Conservation Measures (WD-OECM). Available at: www.protectedplanet.net.

Zawada K, Darling E S, Jupiter S, McClanahan T and Maina J 2026 Global 250 m coral reef prioritization layer v1.0 Zenodo (doi: 10.5281/zenodo.18686274)

Zeng K, He S and Zhan P 2025 Inevitable global coral reef decline under climate change-induced thermal stresses *Commun. Earth Environ.* **6** 827

Zinke J, Gilmour J P, Fisher R et al 2018 Gradients of disturbance and environmental conditions shape coral community structure *Divers. Distrib.* **24** 605–620
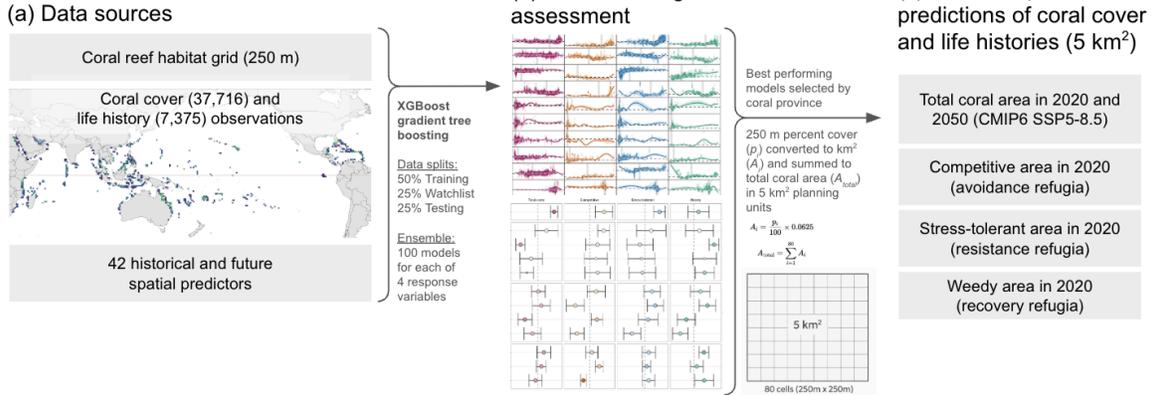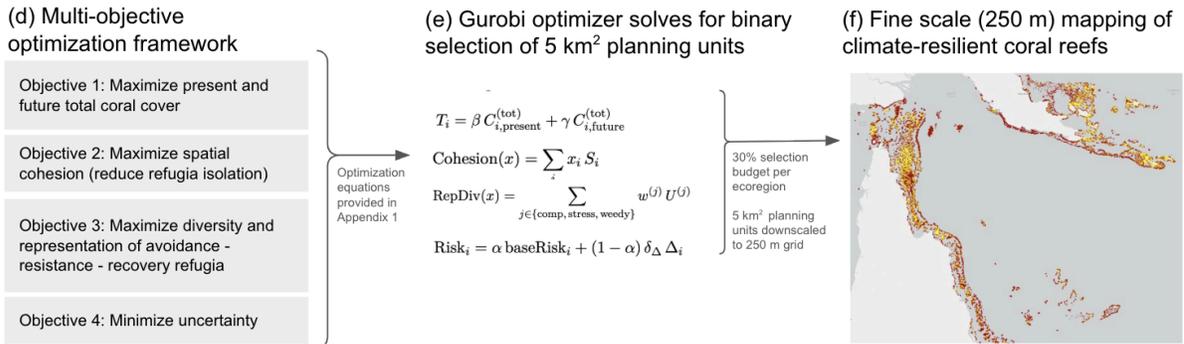
Figure 1. Overview of the analytical workflow used to model global coral cover and life-history composition and to prioritize climate-resilient reef refugia. (a) Coral cover and life-history observations were linked to a 250 m global coral reef habitat grid and 42 historical and future environmental predictors. (b) We trained ensembles of XGBoost gradient-boosted tree models for each response variable, evaluated model performance by coral province, and predicted predicted percent cover of four coral responses at 250 m resolution. (c) Spatial predictions were converted to coral area (km^2) of total coral cover and three life-history types (competitive, stress-tolerant, and weedy) on 5 km^2 grid of planning units. (d) A multi-objective optimization framework was used to identify portfolios of climate refugia that maximize present and future coral area, spatial cohesion, and life-history representation while minimizing uncertainty. Optimization was solved as a binary integer program in Gurobi under a 30 percent per-ecoregion budget. (e) Selected 5 km^2 planning units were downscaled to 250 m to map fine-scale distributions of climate-resilient coral reefs.
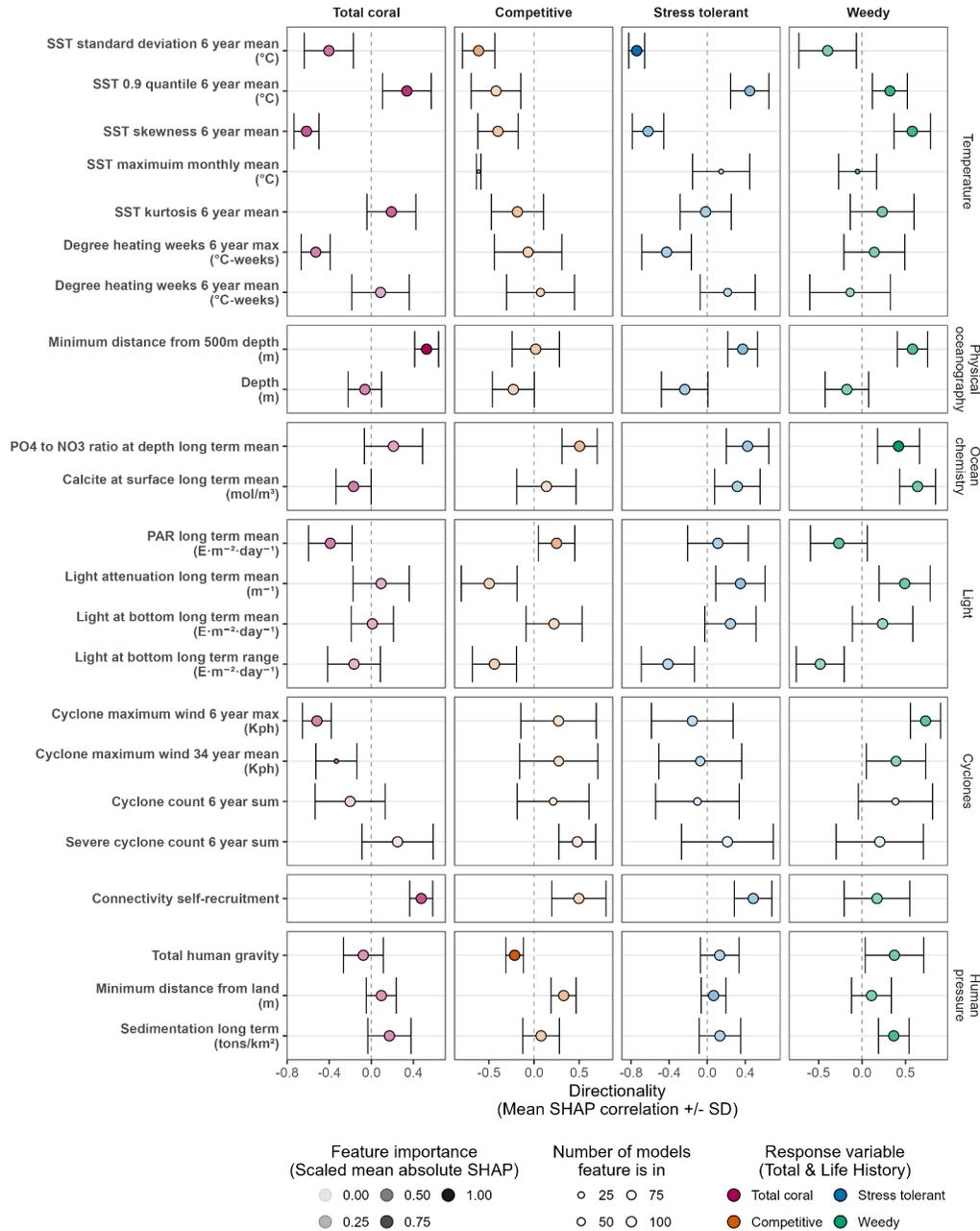
Figure 2. Direction and relative importance of environmental drivers of cover differ among total coral cover and life-history groups. Results are based on 100-model machine-learning ensembles for each response. Correlations represent Pearson coefficients between each predictor and its SHAP contribution to predicted cover. Points show mean correlations across models, with point size indicating the frequency with which each variable was retained after variance-inflation screening. Colour saturation corresponds to feature importance (mean absolute SHAP value). Error bars denote standard deviations, and vertical dashed lines indicate zero correlation. Corresponding response curves and partial dependence plots are provided in Figure S3.

17
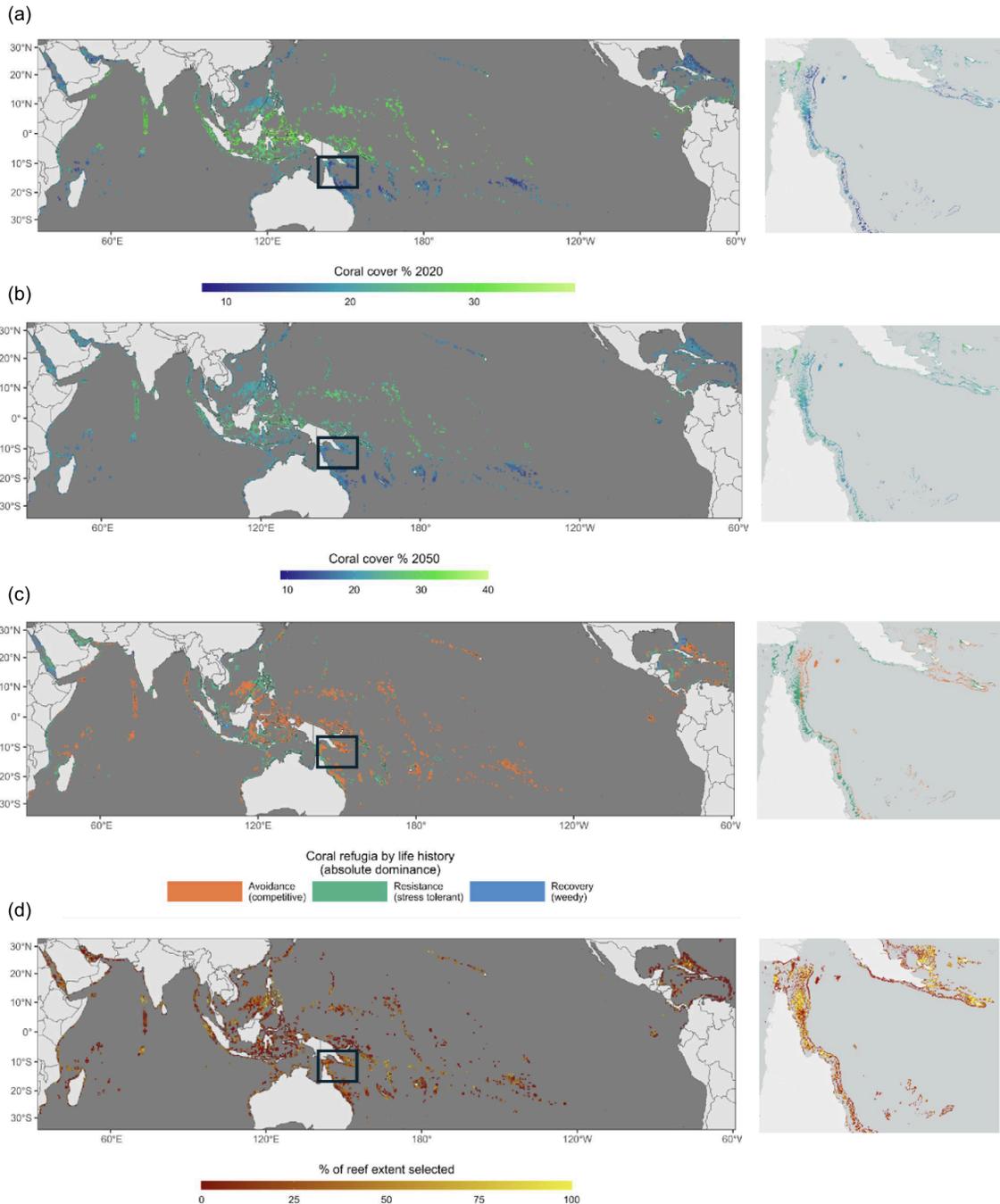
Figure 3. Machine learning and spatial optimization identify contemporary coral refugia from predicted coral cover and life-history composition. (a) Predicted 2020 coral cover from 100-model ensembles. (b) Predicted 2050 cover under CMIP6 SSP5-8.5. (c) Avoidance, resistance, and recovery refugia based on dominant life-history groups. (d) Global prioritization of climate-resilient reefs using a 30% per-ecoregion portfolio that favours high cover, diverse life histories, spatial cohesion, and low ecological risk. Left panels show global patterns at 50 km resolution for visualization of global patterns; right panels illustrate high-resolution examples in the northern Great Barrier Reef and southern Papua New Guinea.

Figure 4. Density plots showing the relative influence of each objective function on prioritization outcomes across marine ecoregions. Distributions represent normalized Z-scores for all planning units within each ecoregion. Grey curves indicate units not selected in the optimization, and red curves indicate units selected in the final 30% portfolios. Overlapping densities illustrate how objective contributions differed between selected and unselected areas and how these patterns varied among ecoregions.

Atlantic Caribbean

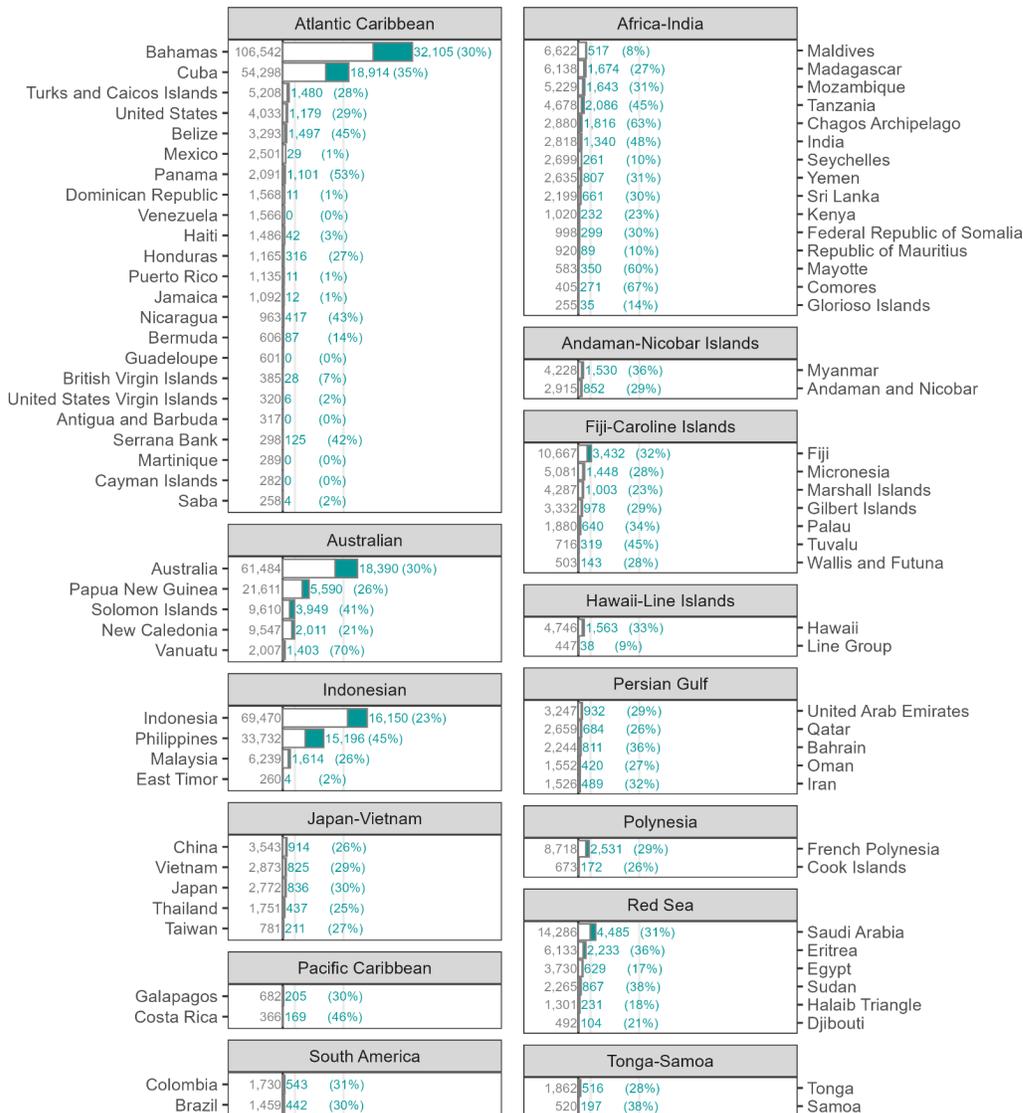|		
Bahamas	106,542	32,105 (30%)
Cuba	54,298	18,914 (35%)
Turks and Caicos Islands	5,208	1,480 (28%)
United States	4,033	1,179 (29%)
Belize	3,293	1,497 (45%)
Mexico	2,501	29 (1%)
Panama	2,091	1,101 (53%)
Dominican Republic	1,568	11 (1%)
Venezuela	1,566	0 (0%)
Haiti	1,486	42 (3%)
Honduras	1,165	316 (27%)
Puerto Rico	1,135	11 (1%)
Jamaica	1,092	12 (1%)
Nicaragua	963	417 (43%)
Bermuda	606	87 (14%)
Guadeloupe	601	0 (0%)
British Virgin Islands	385	28 (7%)
United States Virgin Islands	320	6 (2%)
Antigua and Barbuda	317	0 (0%)
Serrana Bank	298	125 (42%)
Martinique	289	0 (0%)
Cayman Islands	282	0 (0%)
Saba	258	4 (2%)

Australian

Australia	61,484	18,390 (30%)
Papua New Guinea	21,611	5,590 (26%)
Solomon Islands	9,610	3,949 (41%)
New Caledonia	9,547	2,011 (21%)
Vanuatu	2,007	1,403 (70%)

Indonesian

Indonesia	69,470	16,150 (23%)
Philippines	33,732	15,196 (45%)
Malaysia	6,239	1,614 (26%)
East Timor	260	4 (2%)

Japan-Vietnam

China	3,543	914 (26%)
Vietnam	2,873	825 (29%)
Japan	2,772	836 (30%)
Thailand	1,751	437 (25%)
Taiwan	781	211 (27%)

Pacific Caribbean

Galapagos	682	205 (30%)
Costa Rica	366	169 (46%)

South America

Colombia	1,730	543 (31%)
Brazil	1,459	442 (30%)

Africa-India

6,622	517	(8%)	Maldives
6,138	1,674	(27%)	Madagascar
5,229	1,643	(31%)	Mozambique
4,678	2,086	(45%)	Tanzania
2,880	1,816	(63%)	Chagos Archipelago
2,818	1,340	(48%)	India
2,699	261	(10%)	Seychelles
2,635	807	(31%)	Yemen
2,199	661	(30%)	Sri Lanka
1,020	232	(23%)	Kenya
998	299	(30%)	Federal Republic of Somalia
920	89	(10%)	Republic of Mauritius
583	350	(60%)	Mayotte
405	271	(67%)	Comores
255	35	(14%)	Glorioso Islands

Andaman-Nicobar Islands

4,228	1,530	(36%)	Myanmar
2,915	852	(29%)	Andaman and Nicobar

Fiji-Caroline Islands

10,667	3,432	(32%)	Fiji
5,081	1,448	(28%)	Micronesia
4,287	1,003	(23%)	Marshall Islands
3,332	978	(29%)	Gilbert Islands
1,880	640	(34%)	Palau
716	319	(45%)	Tuvalu
503	143	(28%)	Wallis and Futuna

Hawaii-Line Islands

4,746	1,563	(33%)	Hawaii
447	38	(9%)	Line Group

Persian Gulf

3,247	932	(29%)	United Arab Emirates
2,659	684	(26%)	Qatar
2,244	811	(36%)	Bahrain
1,552	420	(27%)	Oman
1,526	489	(32%)	Iran

Polynesia

8,718	2,531	(29%)	French Polynesia
673	172	(26%)	Cook Islands

Red Sea

14,286	4,485	(31%)	Saudi Arabia
6,133	2,233	(36%)	Eritrea
3,730	629	(17%)	Egypt
2,265	867	(38%)	Sudan
1,301	231	(18%)	Halaib Triangle
492	104	(21%)	Djibouti

Tonga-Samoa

1,862	516	(28%)	Tonga
520	197	(38%)	Samoa

Figure 5. Climate refugia for coral reefs are unevenly distributed across coral reef countries and territories. Exclusive Economic Zones (EEZs) define national, territorial, and jurisdictional units, grouped by coral province. Bars show suitable habitat that was selected (blue) or not selected (white), with grey labels indicating total reef extent (km^2). Blue labels show the area of climate resilient reefs and percent of total reef extent. Countries and territories with more than 250 km^2 of reef area are shown; full results are provided in Table S6.

Supporting Information

Machine-learning models of coral cover and life histories reveal that climate refugia for coral reefs persist into 2050

Approach to selecting modeling variables
We included a broad suite of predictor variables spanning climate, chemistry, physical, ecological, and anthropogenic factors. Variables were selected from sources commonly used in coral reef predictive compilations (Table S3). Eight variables characterized recent thermal history over the six years prior to the observation year, and one described long-term mean temperature between 1986 and 2020. Four variables quantified cyclone exposure risk across the full study period and during the six years preceding field observations. Seven variables described larval connectivity among reef habitats based on hydrodynamic modelling. We also included seven water chemistry variables representing long-term mean concentrations of nutrients, trace elements, and related parameters such as pH. Four variables captured incoming light, and four proxies of human pressure represented local stressors. Finally, six moderating variables describing general environmental conditions were included, such as depth, topography, and current velocity, which are likely to interact with other predictors. Although not a predictor per se, coral province was included as a categorical variable to allow response–predictor relationships to vary regionally.

Variables were classified as either time-invariant or time-aware. For a given site across multiple years, some predictors were constant aggregated values, whereas others represented summaries calculated relative to the observation year. For example, mean sea surface temperature (SST) was calculated either as a long-term average (1986–2020) or as a six-year running mean preceding the field observation year. This framework allowed comparison of long-term spatial patterns while also capturing temporal change. A six-year lag period was selected to represent both background environmental conditions and recovery-relevant disturbance windows (Graham et al 2011). Alternative time windows were evaluated using a model uplift approach to optimize coral cover predictions. Where available, forecasted predictors were incorporated to project coral cover under climate change scenarios. Most environmental forecasts were derived from CMIP6 Shared Socio-economic Pathways, including best-case (SSP2-4.5), most-likely (SSP3-7.0), and worst-case (SSP5-8.5) scenarios for 2050 (Eyring et al 2016). These SSP projections represent alternative future trajectories of demographics, economics, technology, and environmental policy, and are used to drive climate model outputs for impact assessment.

Temperature variables
Sea surface temperature summary statistics included annual mean, median, skewness, kurtosis, standard deviation, 5th and 90th percentiles, and minimum and maximum values. These metrics describe both central tendency and extremes and were derived from long-term historical SST (Huang et al 2017), future CMIP6 projections (Eyring et al 2016) at 25 km resolution, and NOAA daily and monthly 5 km SST rasters (Liu et al 2017; Skirving et al 2020). Daily NOAA data were used to construct monthly climatologies for 2000–2010 to capture fine-scale spatial variability. These climatologies were then applied to downscale the 25 km historical and projected datasets to 5 km resolution, preserving spatial and seasonal structure in future predictions.

Mean temperature metrics represent habitat suitability, whereas extremes are associated with bleaching and mortality. Extremely low temperatures may also reduce growth or induce mortality (Burton and Walter 1987). Standard deviation reflects thermal variability, where low variability may increase vulnerability to anomalous events (Carilli et al 2012). Additional derived metrics included degree heating weeks, representing cumulative thermal stress (Liu et al 2014), and SST rate of rise, capturing trends in local warming linked to increased stress risk (Frieler et al 2013). Except for rate of rise, SST variables were calculated over both long-term (1986–2020) and six-year time-aware windows preceding coral cover observations, extending to 2050. The six-year window was selected to represent recent disturbances, while long-term metrics characterized baseline climatology.

Additional climate predictors included long-term rainfall, as intermittent freshwater input may reduce salinity and impair coral growth (Ding et al 2022). Rainfall was derived from bias-corrected MERRA-2 datasets (Reichle et al 2017), representing precipitation averages from 1991 to 2020 at approximately 60 km resolution.

Cyclones
Cyclones can exert both mitigating and destructive effects on coral assemblages. While short-term cooling may reduce thermal stress (Carrigan and Puotinen 2011), intense cyclones are associated with mortality and structural reorganization through hydrodynamic disturbance (Madin and Connolly 2006; Massel and Done 1993). Cyclone exposure was derived from the IBTrACS global cyclone database (Gahtan et al n.d.), which provides historical storm tracks and maximum sustained wind speeds. Annual exposure layers were generated using inverse distance weighting to a 1000 km radius based on the average radius of the outermost closed isobar (ROCI), with wind speeds declining to 20 kph at the edge. Although simplified relative to alternative ROCI estimation methods (Weber et al 2014), this approach enabled global consistency. Wind speed decay calculations were repeated for each track time point, retaining maximum

values where overlaps occurred. Resulting rasters (~200 km resolution at the equator) were used to compute annual maximum wind speeds and cyclone frequency per pixel. Both long-term and six-year mean and maximum summaries were calculated.

Ocean chemistry
Ocean chemistry variables were sourced from Bio-ORACLE 2.0 and 3.0 (Assis et al 2018; Assis et al 2024), including present-day long-term averages and CMIP6 projections. Nutrient variables included iron and calcite, as iron may limit zooxanthellae productivity (Reich et al 2020), and calcite reflects calcium carbonate availability for skeletal growth. Dissolved oxygen was included due to its strong predictive relationship with coral cover (Vercammen et al 2019). pH influences carbonate ion availability (Andersson et al 2009) and acid–base regulation in calcifiers (Cyronak et al 2016), though relationships with coral cover remain context-dependent (Glynn and Manzello 2015; Manzello et al 2021). Salinity was also included, given optimal coral growth near 35 psu and strong interactions with temperature (Ding et al 2022; Ferrier-Pagès et al 1999).

Additional nutrient variables included nitrogen, phosphorous, and their ratio (N:P). Phosphate limitation may increase bleaching susceptibility (Rosset et al 2017), particularly under specific nitrogen conditions (D'Angelo and Wiedenmann 2014). At broader ecological scales, elevated nutrient loads may facilitate algal dominance (Lesser 2021).

Oceanography
Oceanographic predictors included bathymetry and current-related variables. Depth data were obtained from GEBCO (GEBCO Compilation Group 2024). Depth influences coral distribution (Jackson 1979), may provide refuge from bleaching at greater depths (Baird et al 2018), and shapes growth potential via light availability (Dullo 2005). Slope, terrain ruggedness index, and topographic position index described geomorphology, distinguishing lagoons, reef crests, walls, and bommie-dominated habitats. Geomorphology classifications from the Allen Coral Atlas were also included where available (Lyons et al 2020). Distance to the nearest 500 m depth contour was incorporated based on prior evidence linking it to coral cover (McClanahan and Azali 2021).

Light-related predictors included bottom light availability, surface PAR, and diffuse attenuation coefficient from Bio-ORACLE 2.0 (Assis et al 2018). Light regulates coral growth and distribution (Chalker et al 1988; Jackson 1979), though high irradiance combined with elevated temperature can induce bleaching (Lesser 2011). Light

attenuation through the water column influences species zonation and life-history distributions (Jackson 1979).

Larval connectivity

Connectivity among reef patches influences recovery potential via larval supply (Hock et al 2017). Passive larval dispersal models from Fontoura et al (2022) at 8 km × 8 km resolution were used to derive outdegree, indegree, inflow, outflow, netflow, and local retention metrics.

Human pressure and threats

Fishing pressure was represented using human gravity of markets (Cinner et al 2018), calculated as population size divided by squared travel time to reefs. Distance to land was included as a proxy for land-based stressors such as fishing and runoff. Sedimentation can cause mortality and disease (Duckworth et al 2017), and chronic exposure indicates degraded habitat. Sediment plume data from Andrello et al (2022) were used to estimate mean sediment load per reef cell.

References

Andersson A J, Kuffner I B, Mackenzie F T, Jokiel P L, Rodgers K S and Tan A 2009 Net loss of $CaCO_3$ from a subtropical calcifying community due to seawater acidification: mesocosm-scale experimental evidence *Biogeosciences* **6** 1811–23 (doi: 10.5194/bg-6-1811-2009)

Andrello M, Darling E S, Wenger A, Suárez-Castro A F, Gelfand S and Ahmadia G N 2022 A global map of human pressures on tropical coral reefs *Conserv. Lett.* **15** e12858 (doi: 10.1111/conl.12858)

Assis J, Tyberghein L, Bosch S, Verbruggen H, Serrão E A and De Clerck O 2018 Bio-ORACLE v2.0: extending marine data layers for bioclimatic modelling *Glob. Ecol. Biogeogr.* **27** 277–84 (doi: 10.1111/geb.12693)

Assis J, Fernández Bejarano S J, Salazar V W, Schepers L, Gouvêa L, Fragkopoulou E, Leclercq F, Vanhoorne B, Tyberghein L, Serrão E A, Verbruggen H and De Clerck O 2024 Bio-ORACLE v3.0: pushing marine data layers to the CMIP6 Earth System Models of climate change research *Glob. Ecol. Biogeogr.* **33** e13813 (doi: 10.1111/geb.13813)

Baird A H, Madin J S, Álvarez-Noriega M, Fontoura L, Kerry J T, Kuo C-Y, Precoda K, Torres-Pulliza D, Woods R M, Zawada K J A and Hughes T P 2018 A decline in

bleaching suggests that depth can provide a refuge from global warming in most coral taxa *Mar. Ecol. Prog. Ser.* **603** 257–64 (doi: 10.3354/meps12732)

Burton E A and Walter L M 1987 Relative precipitation rates of aragonite and Mg-calcite from seawater: temperature or carbonate ion control? *Geology* **15** 111–14 (doi: 10.1130/0091-7613(1987)15<111:RPROAA>2.0.CO;2)

Carilli J, Donner S D and Hartmann A C 2012 Historical temperature variability affects coral response to heat stress *PLoS One* **7** e34418 (doi: 10.1371/journal.pone.0034418)

Carrigan A D and Puotinen M L 2011 Assessing the potential for tropical-cyclone-induced sea surface cooling to reduce thermal stress on the world's coral reefs *Geophys. Res. Lett.* **38** L23604 (doi: 10.1029/2011GL049722)

Chalker B E, Barnes D J, Dunlap W C and Jokiel P L 1988 Light and reef-building corals *Interdiscip. Sci. Rev.* **13** 222–37 (doi: 10.1179/isr.1988.13.3.222)

Cinner J E *et al* 2018 Gravity of human impacts mediates coral reef conservation gains *Proc. Natl Acad. Sci. USA* **115** E6116–26 (doi: 10.1073/pnas.1708001115)

Cyronak T, Schulz K G and Jokiel P L 2016 The omega myth: what really drives lower calcification rates in an acidifying ocean *ICES J. Mar. Sci.* **73** 558–62 (doi: 10.1093/icesjms/fsv075)

D'Angelo C and Wiedenmann J 2014 Impacts of nutrient enrichment on coral reefs: new perspectives and implications for coastal management and reef survival *Curr. Opin. Environ. Sustain.* **7** 82–93 (doi: 10.1016/j.cosust.2013.11.029)

Ding D-S, Patel A K, Singhania R R, Chen C-W and Dong C-D 2022 Effects of temperature and salinity on growth, metabolism and digestive enzyme synthesis of *Goniopora columna Biology (Basel)* **11** 436 (doi: 10.3390/biology11030436)

Duckworth A, Giofre N and Jones R 2017 Coral morphology and sedimentation *Mar. Pollut. Bull.* **125** 289–300 (doi: 10.1016/j.marpolbul.2017.08.036)

Dullo W-C 2005 Coral growth and reef growth: a brief review *Facies* **51** 33–48 (doi: 10.1007/s10347-005-0060-y)

Eyring V, Bony S, Meehl G A, Senior C A, Stevens B, Stouffer R J and Taylor K E 2016 Overview of the Coupled Model Intercomparison Project Phase 6 (CMIP6) experimental design and organization *Geosci. Model Dev.* **9** 1937–58 (doi: 10.5194/gmd-9-1937-2016)

Ferrier-Pagès C, Gattuso J-P and Jaubert J 1999 Effect of small variations in salinity on the rates of photosynthesis and respiration of *Stylophora pistillata Mar. Ecol. Prog. Ser.* **181** 309–14 (doi: 10.3354/meps181309)

Fontoura L, D'Agata S, Gamoyo M, Barneche D R, Luiz O J, Madin E M P, Eggertsen L and Maina J M 2022 Protecting connectivity promotes successful biodiversity and fisheries conservation *Science* **375** 336–40 (doi: 10.1126/science.abg4351)

Frieler K, Meinshausen M, Golly A, Mengel M, Lebek K, Donner S D and Hoegh-Guldberg O 2013 Limiting global warming to 2 °C is unlikely to save most coral reefs *Nat. Clim. Change* **3** 165–70 (doi: 10.1038/nclimate1674)

Gahtan J, Knapp K R, Schreck J I, Diamond H J, Kossin J P and Kruk M C n.d. International Best Track Archive for Climate Stewardship (IBTrACS) Project, Version 4.01 NOAA Natl. Centers Environ. Inf.

GEBCO Compilation Group 2024 GEBCO 2024 Grid (doi: 10.5285/1c44ce99-0a0d-5f4f-e063-7086abc0ea0f)

Glynn P W and Manzello D P 2015 Bioerosion and coral reef growth: a dynamic balance *Coral Reefs in the Anthropocene* (Dordrecht: Springer) pp 67–97 (doi: 10.1007/978-94-017-7249-5_4)

Graham N A J, Nash K L and Kool J T 2011 Coral reef recovery dynamics in a changing world *Coral Reefs* **30** 283–94 (doi: 10.1007/s00338-010-0717-z)

Hock K, Wolff N H, Ortiz J C, Condie S A, Anthony K R N, Blackwell P G and Mumby P J 2017 Connectivity and systemic resilience of the Great Barrier Reef *PLoS Biol.* **15** e2003355 (doi: 10.1371/journal.pbio.2003355)

Huang B *et al* 2017 Extended reconstructed sea surface temperature, version 5 (ERSSTv5): upgrades, validations and intercomparisons *J. Clim.* **30** 8179–205 (doi: 10.1175/JCLI-D-16-0836.1)

Jackson J B C 1979 Morphological strategies of sessile animals *Biol. Syst. Colonial Animals* (New York: Academic Press) pp 499–555

Lesser M P 2011 Coral bleaching: causes and mechanisms *Coral Reefs: An Ecosystem in Transition* (Dordrecht: Springer) pp 405–19 (doi: 10.1007/978-94-007-0114-4_23)

Lesser M P 2021 Eutrophication on coral reefs: evidence for phase shifts, nutrient limitation and coral bleaching *BioScience* **71** 1216–33 (doi: 10.1093/biosci/biab101)

Liu G *et al* 2014 Reef-scale thermal stress monitoring of coral ecosystems: new 5-km global products from NOAA Coral Reef Watch *Remote Sens.* **6** 11579–606 (doi: 10.3390/rs61111579)

Liu G, Skirving W J, Geiger E F, Heron S F, Tirak K V, Strong A E and Eakin C M 2017 NOAA Coral Reef Watch's 5-km satellite coral bleaching heat stress monitoring product suite version 3 and four-month outlook version 4 *NOAA Tech. Rep.* **32**

Lyons M B *et al* 2020 Mapping the world's coral reefs using a global multiscale earth-observation framework *Remote Sens. Ecol. Conserv.* **6** 557–68 (doi: 10.1002/rse2.157)

Madin J S and Connolly S R 2006 Ecological consequences of major hydrodynamic disturbances on coral reefs *Nature* **444** 477–80 (doi: 10.1038/nature05328)

Manzello D P, Enochs I C, Carlton R, Bruckner A, Kolodziej G, Dempsey A and Renaud P 2021 Pacific-wide pH snapshots reveal that high coral cover correlates with low but variable pH *Bull. Mar. Sci.* **97** 239–56 (doi: 10.5343/bms.2019.0100)

Massel S R and Done T J 1993 Effects of cyclone waves on massive coral assemblages on the Great Barrier Reef: meteorology, hydrodynamics and demography *Coral Reefs* **12** 153–66

McClanahan T R and Azali M K 2021 Environmental variability and threshold model predictions for coral reefs *Front. Mar. Sci.* **8** —

Reich H G, Rodriguez I B, LaJeunesse T C and Ho T-Y 2020 Endosymbiotic dinoflagellates pump iron: differences in iron and trace-metal needs among the Symbiodiniaceae *Coral Reefs* **39** 915–27 (doi: 10.1007/s00338-020-01911-z)

Reichle R H, Liu Q, Koster R D, Draper C S, Mahanama S P P and Partyka G S 2017 Land surface precipitation in MERRA-2 *J. Clim.* **30** 1643–66 (doi: 10.1175/JCLI-D-16-0570.1)

Rosset S, Wiedenmann J, Reed A J and D'Angelo C 2017 Phosphate deficiency promotes coral bleaching and is reflected by the ultrastructure of symbiotic dinoflagellates *Mar. Pollut. Bull.* **118** 180–87 (doi: 10.1016/j.marpolbul.2017.02.044)

Skirving W, Marsh B, De La Cour J, Liu G, Harris A, Maturi E, Geiger E and Eakin C M 2020 CoralTemp and the Coral Reef Watch Coral Bleaching Heat Stress Product Suite version 3.1 *Remote Sens.* **12** 3856 (doi: 10.3390/rs12233856)

Vercammen A, McGowan J, Knight A T, Pardede S, Muttaqin E, Harris J, Ahmadia G, Estradivari, Dallison T, Selig E and Beger M 2019 Evaluating the impact of accounting for coral cover in large-scale marine conservation prioritizations *Divers. Distrib.* **25** 1564–74 (doi: 10.1111/ddi.12957)

Weber H C, Lok C C F, Davidson N E and Xiao Y 2014 Objective estimation of the radius of the outermost closed isobar in tropical cyclones *Trop. Cyclone Res. Rev.* **3** 1–21 (doi: 10.6057/2014TCRR01.01)
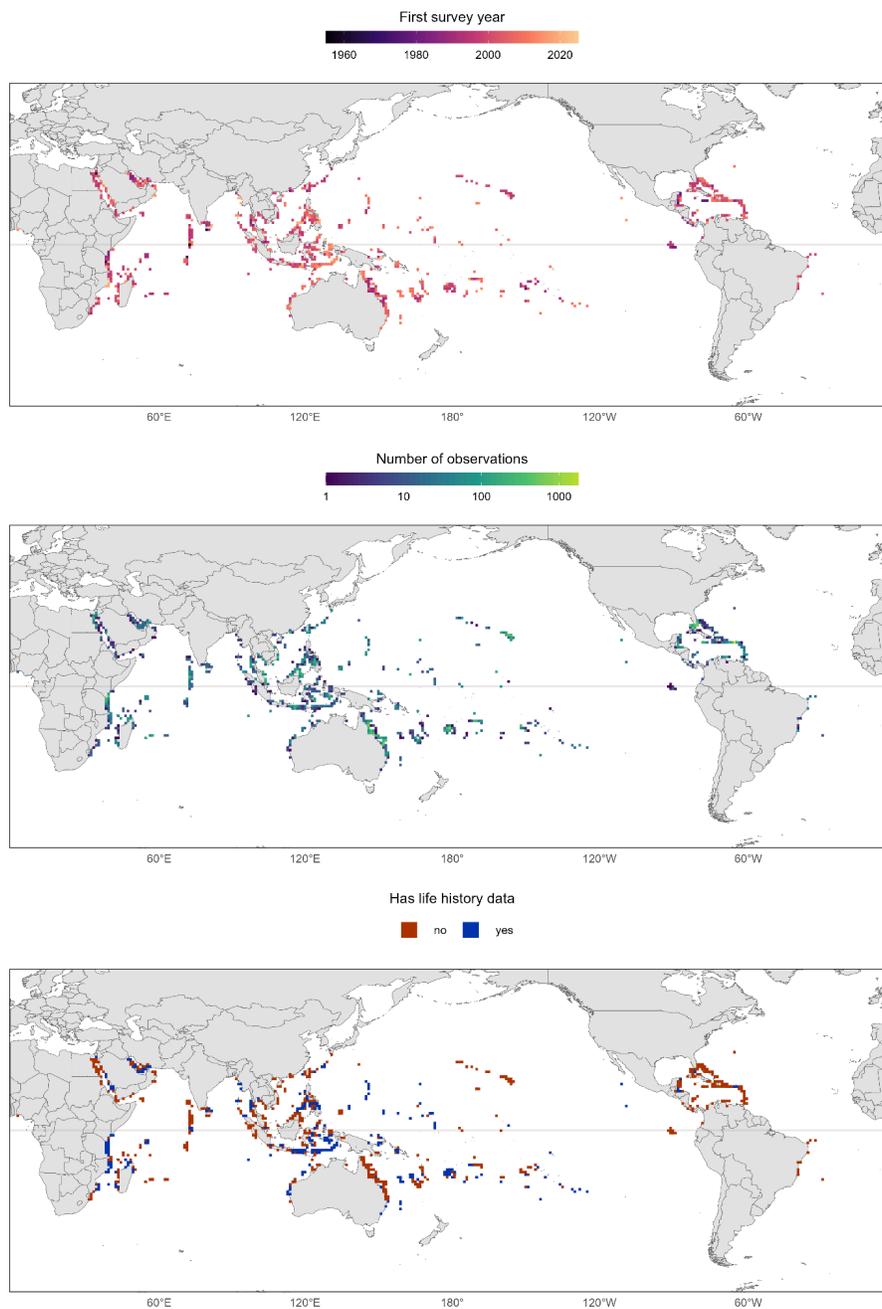
Figure S1. Global coverage of compiled coral observations from 37,716 unique coral cover records. Panels show: (top) first survey year at each location, (middle) number of observations per location as an indicator of sampling effort, and (bottom) locations with and without available coral life history data. For visualization, data are gridded at 1° spatial resolution (approximately 111 km at the equator).
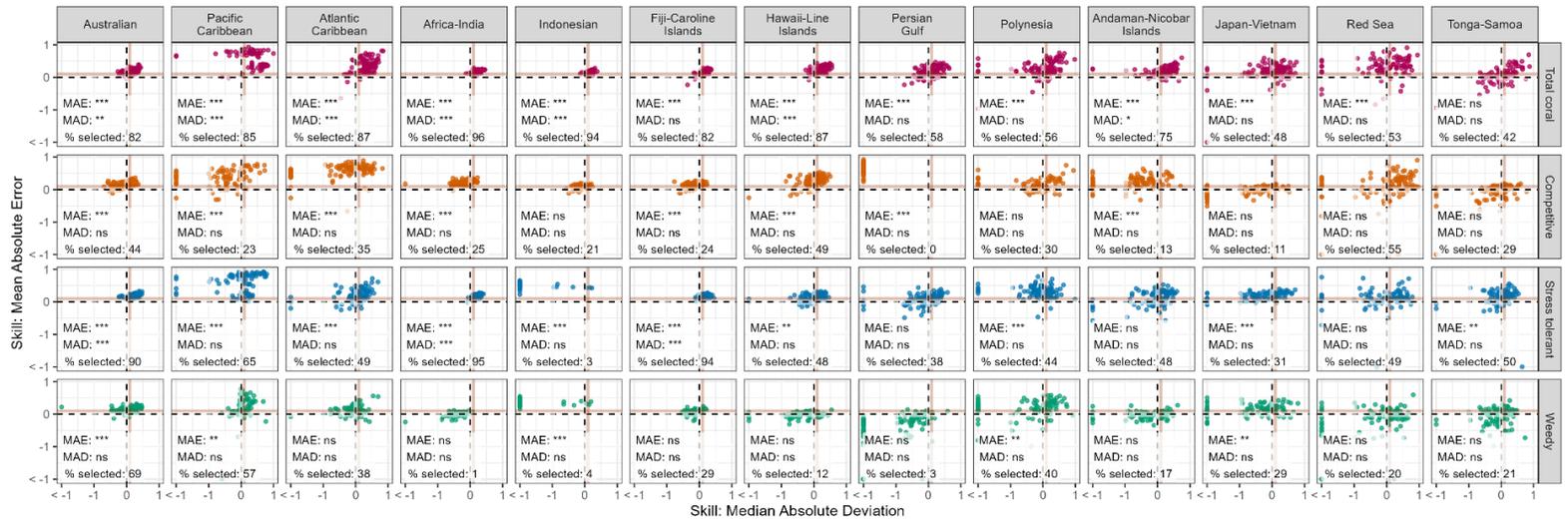
Figure S2. Model skill for predicting total coral cover and life-history cover, shown as mean absolute error (MAE) skill (y-axis) and median absolute deviation (MAD) skill (x-axis), evaluated against a mean-only null model. Skill is defined as *skill = 1 – (error_model / error_null)*, computed separately for MAE and MAD, where values > 0 (dashed lines) indicate improvement over the null model. Higher MAE skill indicates lower overall absolute error on test data, and higher MAD skill reflects reduced dispersion of errors. Each point represents the skill scores for one model run. Significance stars summarise one-sided Monte Carlo permutation tests across 100 runs per response per province, testing whether skill exceeds a practical threshold of 0.1 (≥10% improvement; solid lines): *** p < 0.001, ** p < 0.01, * p < 0.05, *ns* p ≥ 0.05. Each response variable includes 100 globally trained model runs, with performance summarised at the province level. Coral provinces are ordered left to right from lowest to highest joint p-value. Negative skill values are rounded up for visual clarity.
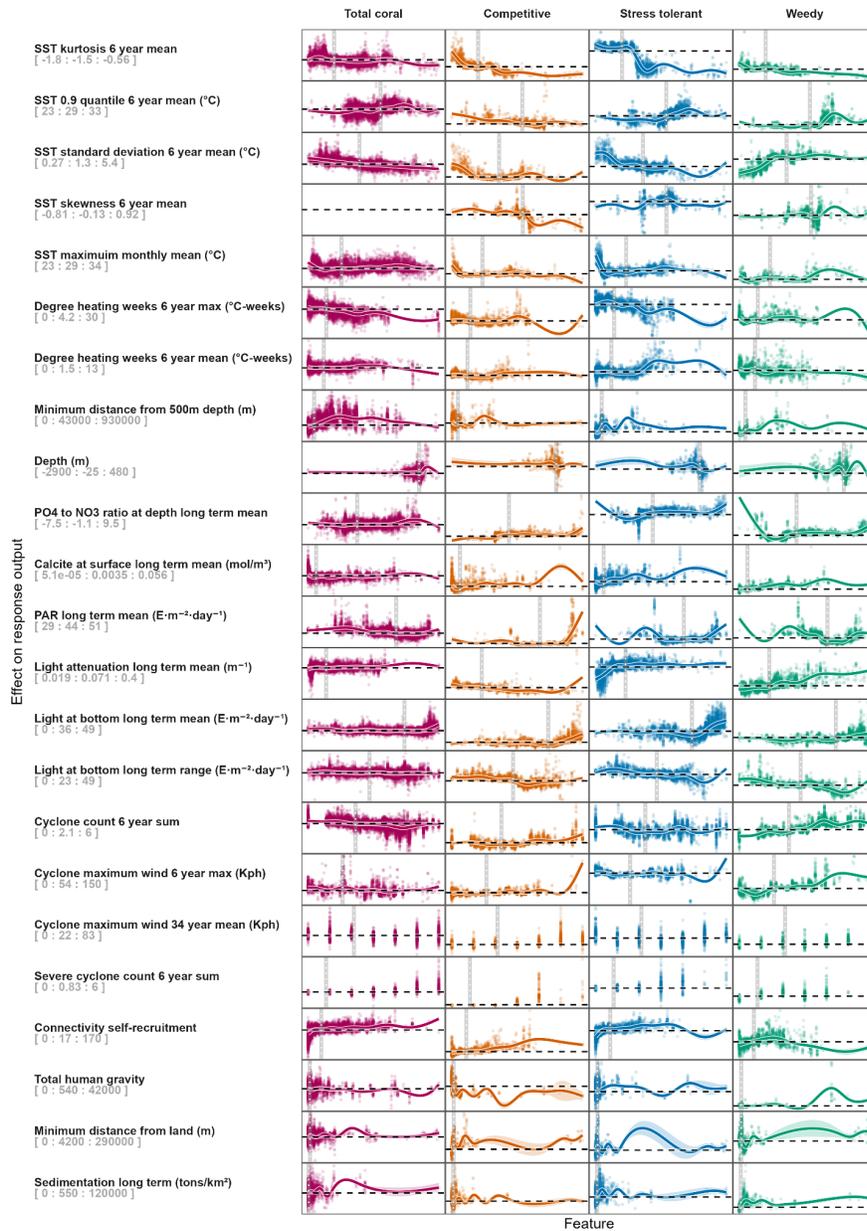
Figure S3. Conditional partial plots showing variable influence on total and life-history coral cover. Y-axis values represent SHAP effects of each variable on predicted outcomes, with dashed lines at 0 indicating no effect. Vertical grey bars show mean variable values; minimum, mean, and maximum values are listed beneath each variable. Points show mean SHAP values across 100 models for each training point, and lines show generalized additive models (10 knots, thin-plate spline basis) weighted by SHAP variability. Partials reflect effects conditional on all other predictors, so responses may depend on the local predictor context. Axes are scaled freely to highlight relationship shapes; overall importance and directionality are shown in Figure 2 of the main text.
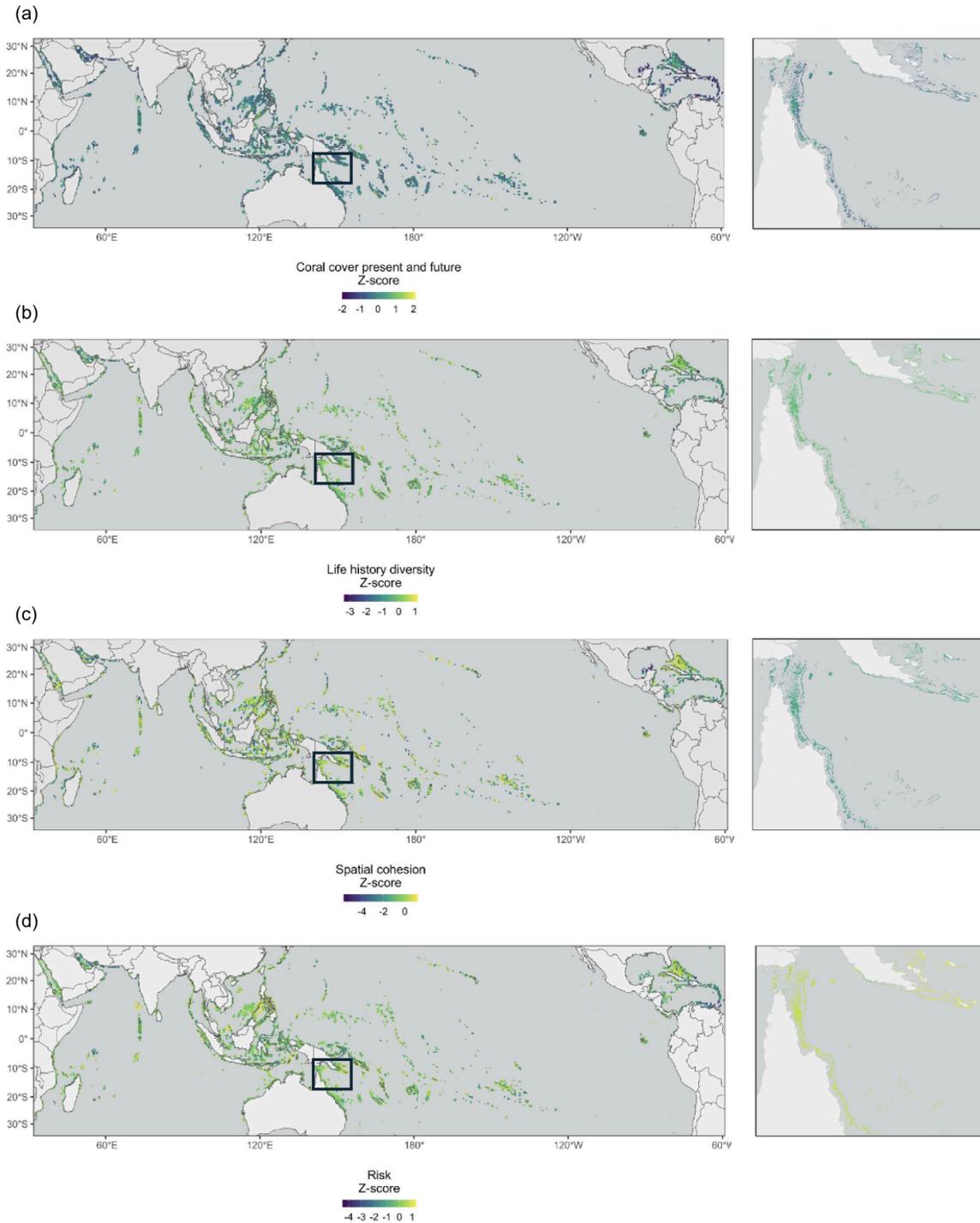
Figure S4. Spatial variation in Z-scores for the four objectives used in the climate resilient reef prioritization. These maps illustrate how the relative strength of each objective varies across regions, providing insight into how sensitive prioritization outcomes are to underlying ecological and environmental gradients. (A) Coral cover (2020 and 2050). (B) Life-history diversity. (C) Spatial cohesion. (D) Risk. Left panels show global 50-km visualization; right panels show examples at full model resolution in the northern Great Barrier Reef and southern Papua New Guinea.

Description of Supplementary Tables and Appendix

Table S1. Coral reef observation datasets used for model training and validation. Each dataset is summarised by the number of observations, availability of life history data, temporal coverage (first and last observation year), and full citation. These datasets provide the empirical basis for modelling coral cover and life-history composition across global reef systems.

Table S2. Life-history trait assignments for coral taxa. Coral genera and species were classified into competitive, stress-tolerant, and weedy life-history strategies, with some taxa allocated proportionally across groups to reflect variation in morphology and ecological behaviour (e.g. branching vs. massive forms). These proportional assignments were used to derive life-history composition for all modelling analyses.

Table S3. Predictor variables (n = 42) used in coral-cover and life-history models. For each environmental and anthropogenic variable, the table reports a brief description, units, spatial and temporal resolution, and source dataset.

Table S4. Training and testing performance of machine-learning models predicting total coral cover and life-history group cover. Metrics include mean R^2 and mean absolute error (MAE) across 100 model runs (± SD). High training R^2 values indicate strong within-sample fits, while lower testing R^2 and higher MAE values reflect the challenge of predicting fine-scale coral cover patterns under real-world variability. Life-history models generally show lower predictive skill than total coral cover, consistent with greater noise and fewer observations in taxonomically resolved datasets.

Table S5. Regional model performance and selection criteria for coral-cover predictions. For each coral province, the table reports skill metrics (mean absolute error skill and median absolute deviation skill), their variability (SD), and one-sided permutation test p-values assessing improvement over a null model. Columns also show the proportion of models from the global pool meeting predefined MAE and MAD thresholds, and the percentage meeting both criteria. Models passing both thresholds were retained for regional ensemble predictions of 2020 and 2050 coral cover.

Table S6. Spatial optimization outcomes by countries, territories and jurisdictions. For each coral reef area, we estimate total reef extent and the area selected as climate-resilient refugia under the 50 Reefs plus optimisation, including the proportion of newly identified priority area and the overlap with the original Beyer et al. (2018) prioritisation. Values for areas selected only by Beyer et al., as well as reef habitat not selected by either approach, are provided in km^2 and as percentages of total reef extent.

Appendix S1. Gurobi solver equations and configurations. This appendix outlines the mathematical formulation of the spatial optimization problem and the Gurobi-specific settings used to obtain stable, spatially coherent solutions.

Objective Functions with Descriptors

2026-01-27

Objective 1: Temporal Return

Per-pixel temporal return: blend of present and future absolute total cover (m^2).

$$T_i = \beta\, C_{i,\text{present}}^{(\text{tot})} + \gamma\, C_{i,\text{future}}^{(\text{tot})}, \quad \beta + \gamma = 1 \tag{1}$$

Where:

- T_i — temporal return for pixel i (m^2-weighted).

- $C_{i,\text{present}}^{(\text{tot})}$ — present absolute total cover in pixel i (m^2).

- $C_{i,\text{future}}^{(\text{tot})}$ — future absolute total cover in pixel i (m^2).

- $\beta,\ \gamma$ — weights on present and future, respectively, with $eta + \gamma = 1$.

Portfolio temporal return as the sum over selected pixels.

$$R(x) = \sum_i x_i\, T_i \tag{2}$$

Where:

- $R(x)$ — portfolio return for selection vector x.

- x_i — binary decision (1 if pixel i is selected; 0 otherwise).

- T_i — per-pixel temporal return.

Objective 2: Spatial Cohesion (kNN with Exponential Decay)

Exponential proximity weights using local distance scale σ_i (median neighbour distance).

$$w_{ik} = \exp\left(-\frac{d_{ik}}{\sigma_i}\right) \tag{3}$$

Where:

- w_{ik} — proximity weight between pixel i and its k-th nearest neighbour.

- d_{ik} — Euclidean distance between pixel i and neighbour k (projected units).

- σ_i — local scale = median distance to neighbours for pixel i.

Per-pixel cohesion as the mean of proximity weights over K neighbours.

$$S_i = \frac{1}{K} \sum_{k=1}^{K} w_{ik} \tag{4}$$

Where:

- S_i — cohesion score for pixel i (unitless).

- K — number of nearest neighbours (≤ 30).

- w_{ik} — proximity weight to neighbour k.

Portfolio cohesion as a linear sum of per-pixel cohesion over selected pixels.

$$\text{Cohesion}(x) = \sum_{i} x_i \, S_i \tag{5}$$

Where:

- $\text{Cohesion}(x)$ — portfolio cohesion score.

- x_i — binary selection for pixel i.

- S_i — per-pixel cohesion score.

Objective 3: Trait Representation and Diversification (Portfolio Level)

Portfolio coverage by trait j from the sum of absolute cover across selected pixels.

$$H^{(j)}(x) = \sum_{i} x_i \, C^{(j)}_{i,\text{present}} \tag{6}$$

Where:

- $H^{(j)}(x)$ — represented area of trait j in the portfolio (m^2).

- $C^{(j)}_{i,\text{present}}$ — present absolute cover of trait j in pixel i (m^2).

- x_i — binary selection for pixel i.

Concave utility (square-root) with smoothing *arepsilon* to produce diminishing returns.

$$U^{(j)} = \sqrt{H^{(j)}(x) + \varepsilon} \tag{7}$$

Where:

- $U^{(j)}$ — utility contributed by trait j.

- $H^{(j)}(x)$ — represented area of trait j (m^2).

- ε — small smoothing constant (e.g., 1 m^2).

Presence (density-based) and rarity weighting per trait within ecoregions.

$$I_i^{(j)} = \mathbf{1}\left\{ D_{i,\text{present}}^{(j)} > \theta \max_k D_{k,\text{present}}^{(j)} \right\}, \quad q^{(j)} = 1 - \frac{\sum_i I_i^{(j)}}{N} \tag{8}$$

Where:

- $I_i^{(j)}$ — indicator (1 if trait j is present in pixel i; 0 otherwise).

- $D_{i,\text{present}}^{(j)}$ — density of trait j in pixel i (m^2 per m^2).

- θ — presence threshold as a fraction of the ecoregion's max trait density.

- $q^{(j)}$ — rarity weight $= 1 - (\sum_i I_i^{(j)})/N$.

Rarity-weighted concave utility summed across traits (single objective, not additive metrics).

$$\text{RepDiv}(x) = \sum_{j \in \{\text{comp, stress, weedy}\}} w^{(j)} U^{(j)} \tag{9}$$

Where:

- $\text{RepDiv}(x)$ — portfolio-level representation/diversification objective.

- $w^{(j)}$ — trait weight (equal or rarity-weighted via $q^{(j)}$).

- $U^{(j)}$ — concave utility for trait j.

Objective 4: Risk

Present uncertainty as a CV-style ratio with a +1 stability offset.

$$r_{i,p}^{(\text{tot})} = \frac{\sigma_{i,p}^{(\text{tot})}}{C_{i,p}^{(\text{tot})} + 1} \tag{10}$$

Where:

- $r_{i,p}^{(\text{tot})}$ — present uncertainty score for pixel i.

- $\sigma_{i,p}^{(\text{tot})}$ — Standard Deviation of present predictions for total cover in pixel i (m^2).

- $C_{i,p}^{(\text{tot})}$ — present absolute total cover in pixel i (m^2); +1 prevents blow-up near zero.

Future uncertainty as a Coefficient of Variation -style ratio with a +1 stability offset.

$$r_{i,f}^{(\text{tot})} = \frac{\sigma_{i,f}^{(\text{tot})}}{C_{i,f}^{(\text{tot})} + 1} \tag{11}$$

Where:

- $r_{i,f}^{(\text{tot})}$ — future uncertainty score for pixel i.

- $\sigma_{i,f}^{(\text{tot})}$ — SD of future predictions for total cover in pixel i (m^2).

- $C_{i,f}^{(\text{tot})}$ — future absolute total cover in pixel i (m^2); +1 prevents blow-up near zero.

Base uncertainty from present/future combined via root-mean-square (RMS).

$$\text{baseRisk}_i = \sqrt{\frac{\left(r_{i,p}^{(\text{tot})}\right)^2 + \left(r_{i,f}^{(\text{tot})}\right)^2}{2}} \tag{12}$$

Where:

- baseRisk_i — combined uncertainty for pixel i (unitless).

- $r_{i,p}^{(\text{tot})}$, $r_{i,f}^{(\text{tot})}$ — present and future uncertainty scores.

Proportional decline from present to future; gains clipped at zero; denominator floored at 1 m^2.

$$\Delta_i = \max\left(\frac{C_{i,p}^{(\text{tot})} - C_{i,f}^{(\text{tot})}}{\max\left(C_{i,p}^{(\text{tot})},\ 1\ \text{m}^2\right)},\ 0\right) \tag{13}$$

Where:

- Δ_i — proportional decline penalty for pixel i (unitless).

- $C_{i,p}^{(\text{tot})}$, $C_{i,f}^{(\text{tot})}$ — present and future absolute total cover (m^2).

- $\max(C_{i,p}^{(\text{tot})},\ 1\ \text{m}^2)$ — denominator floor for numerical stability.

Per-pixel risk as a convex mixture of base uncertainty and decline.

$$\text{Risk}_i = \alpha\,\text{baseRisk}_i + (1 - \alpha)\,\delta_\Delta\,\Delta_i \tag{14}$$

Where:

- Risk_i — per-pixel risk score (unitless).

- α — weight on uncertainty vs. decline (default 0.7).

- δ_Δ — scaling factor for decline penalty (default 1).

- baseRisk_i — combined present/future uncertainty.

- Δ_i — proportional decline penalty.

Portfolio risk as a linear sum of per-pixel risks over selected pixels.

$$\text{Risk}(x) = \sum_i x_i\,\text{Risk}_i \tag{15}$$

Where:

- $\text{Risk}(x)$ — portfolio risk for selection vector x.

- x_i — binary selection for pixel i.

- Risk_i — per-pixel risk score.